

***In-situ* X-ray Diffraction Study of Electric Field Induced Domain Switching and Phase Transition in PZT-5H**

Ming Liu[†], K Jimmy Hsia^{†*}, and Mauro Sardela, Jr.[‡]

Department of Theoretical and Applied Mechanics, University of Illinois at Urbana-
Champaign, Urbana, IL 61801

Center for Microanalysis of Materials, Frederick Seitz Materials Research Laboratory,
University of Illinois at Urbana-Champaign, Urbana, IL 61801

* Corresponding author. Tel.: +1-217-333-2321; fax: +1-217-244-5707.

E-mail: kj-hsia@uiuc.edu

[†] Department of Theoretical and Applied Mechanics

[‡] Frederick Seitz Materials Research Laboratory

Abstract

In-situ x-ray experiments were conducted to examine the electric-field-induced phase changes in PZT-5H materials. The x-ray diffraction profiles at different electric field levels were analyzed by peak fitting and used to identify the occurrence of non-180° domain switching and phase transition. We found that, in depolarized samples, there exists a threshold electric field for the phase changes; whereas in polarized samples, no such threshold exists. The profound difference in the diffraction profile changes under positive and negative electric fields in polarized samples is responsible for the asymmetry of piezoelectric effects. Peak fitting results show composition and transition of phases as well as domain switching at different electric field levels. These observations further indicate the importance of residual stresses in materials behaviors.

I. Introduction

Perovskite ferroelectric/piezoelectric $\text{PbZr}_{1-x}\text{Ti}_x\text{O}_3$ (PZT), $(1-x)\text{Pb}(\text{Mg}_{1/3}\text{Nb}_{2/3})\text{O}_3-x\text{PbTiO}_3$ (PMN-PT) and $(1-x)\text{Pb}(\text{Zn}_{1/3}\text{Nb}_{2/3})\text{O}_3-x\text{PbTiO}_3$ (PZN-PT) have been intensively studied recently. Above the Curie temperature, they all have simple cubic structures, while at lower temperatures, it was believed that they become tetragonal or rhombohedral structures. The composition, x , determines whether a tetragonal or rhombohedral structure is formed at a given temperature. The phase boundary in the phase diagram, which separates tetragonal from rhombohedral region is called the morphotropic phase boundary (MPB)¹. Recently, Noheda et al. reported a new phase in polycrystalline PZT materials, which belongs to one type of monoclinic phases²⁻⁴. They suggested that the MPB that was previously believed to separate tetragonal and rhombohedral phases is actually the boundary between tetragonal and monoclinic phases. They also suggested there exist a “morphotropic phase” region between tetragonal and rhombohedral regions in the phase diagram³. The new monoclinic phase was also observed by Souza Filho et al.⁵.

Extraordinarily strong piezoelectric constants are found mostly in materials with compositions near the MPB. Although the large piezoelectric constants are normally believed to be due to the coexistence of morphotropic phases and the associated phase changes, the underlying mechanisms remain unsettled⁶⁻¹³. On the other hand, it has been found that piezoelectric constants exhibit a large nonlinear behavior¹⁴⁻¹⁸. Above a threshold electric field, the piezoelectric constant increases if the amplitude of the applied electric field increases. The threshold level can be very low or nearly zero^{15,16}, or can be a finite value¹⁷. It was also observed that the piezoelectric constant depends on the

direction of a biased electric field, a positive biased electric field results in decreased piezoelectric constants, while a negative biased field results in increased piezoelectric constants¹⁸. The nonlinear effect was explained by different mechanisms, such as domain wall motion, 90°-domain switching, or residual stresses. However, most of the mechanisms are indirectly deduced from the measurements of material's constants. Only a few direct observations on microstructural changes have been made, especially in the case of polycrystalline materials.

Experiments on single crystalline relaxor-based ferroelectric PMN-PT and PZN-PT showed that enhanced and nonlinear piezoelectric coefficients are likely due to the phase transition between rhombohedral and tetragonal phases induced by electric fields¹⁹⁻²⁰. A first principle simulation indicated that the phase transition results from an electric field induced polarization rotation²¹. Quantitative experiments on polycrystalline materials are difficult to conduct due to their complex microstructures. However, such experiments can help to identify the mechanisms responsible for the enhanced and nonlinear piezoelectric constants. An x-ray diffraction conducted on polycrystalline PZN-PZT indicated that a large amount of phase transitions between rhombohedral and tetragonal phases and non-180° domain switching (90° domain switching for tetragonal phases and 71° or 109° domain switching for rhombohedral phases) are induced by the poling process⁸. However, the result does not provide a direct observation of microstructural changes in a poled sample upon an applied electric field.

PZT-5H is one of the most used polycrystalline PZT materials. Its piezoelectric constants have been studied in detail^{16,22}. Some researchers suggested that tetragonal and rhombohedral phases coexist at room temperatures in the PZT materials with

compositions near the MPB^{16,23,24}. Non-180° domain switching and phase transition between those two phases, therefore, were believed to be the source of their strong, nonlinear piezoelectric behavior¹⁵. Other researchers suggested that residual stresses are the real source¹⁶. The recently modified MPB suggested the coexistence of tetragonal and monoclinic phases in PZT materials near the MPB^{3,4}. Some first-principle simulations, however, suggested that the large piezoelectric effects could come from field-induced monoclinic distortions^{25,26}. A direct observation seems to provide some evidence for such distortions¹¹. But more careful and thorough experiments are needed to confirm the type of those distortions. Therefore, direct observations of electric field induced microstructural changes are critical to clarify the mechanisms responsible for the strong and nonlinear behavior in polycrystalline piezoelectric materials.

In the present paper, *in-situ* x-ray diffraction experiments were performed on a PZT-5H material. Direct observations of non-180° domain switching and phase transition at different electric fields were made for depolarized and polarized samples. Our results provide specific information on the microstructural changes giving rise to the material's piezoelectric properties, and show the effect of residual stresses on the nonlinear piezoelectric behavior.

II. Experiment

Thin plate specimens of PZT-5H are used in our experiments. The samples have a thickness of 375 μm and in-plane dimensions of 2 cm \times 2 cm. The Curie temperature of the material is 220 °C and the coercive field (E_C) is 8 KV/cm. All samples are coated with nickel as electrodes on the top and bottom surfaces and poled in their thickness

directions. Some samples were depolarized by submerging them into a silicon–oil bath at 260 °C for half an hour, and then cooling down to room temperature gradually. The diffraction patterns of the depolarized samples are close to those of ceramic powder.

Recent research suggested that PZT-5H could have a combination of tetragonal and rhombohedral phases¹⁶ or a combination of tetragonal and monoclinic phases^{3,4}. Figure 1 shows the geometries of a tetragonal, a rhombohedral, and a monoclinic unit cell. The lattice angle α for a rhombohedral unit cell is slightly less than 90°. The monoclinic unit cell is double in volume compared to a tetragonal unit cell. Its a_m and b_m lie along the tetragonal $[\bar{1}\bar{1}0]$ and $[1\bar{1}0]$ directions, respectively. Its c_m tilts slightly from the $[001]$ direction with the angle β between a_m and c_m slightly larger than 90°. The polarization directions are along (001) and (111) for tetragonal and rhombohedral unit cells, respectively. The polarization direction can lie anywhere between (001) and (101) in $a_m c_m$ plane for a monoclinic unit cell.

The x-ray diffraction (2θ - θ scan) is performed with a Rigaku D-Max powder x-ray diffractometer at the Frederick Seitz Materials Research Laboratory at the University of Illinois. The instrument uses copper radiation with lines $K\alpha_1$ and $K\alpha_2$ (wavelength $\lambda_{\alpha_1} = 1.5406 \text{ \AA}$ and $\lambda_{\alpha_2} = 1.5444 \text{ \AA}$). The top and bottom electrodes of the samples are connected to a DC power supply. The x-ray diffraction is measured *in-situ* under applied electric fields. Because of their morphotropic and polycrystalline microstructures, diffraction patterns are rather complicated. A moderate-speed scan is first conducted for a large 2θ range to locate approximately the peak positions. Slow scans are then conducted for individual peaks in a 3°-4° 2θ range. The effect of the electric field on diffraction

peaks is studied first. Domain and phase changes are further studied by peak fitting. Those peaks are carefully fitted by a peak fitting program Xfit-Koalariet developed by Cheary and Coelho²⁷. The peaks are fitted by a pseudo-Voigt (PV) shape function and the two-wavelength effect is taken into account. Furthermore, the anisotropic peak width and coexisting phases are also considered^{3,4}.

III. Results and Discussions

3.1 Effect of Electric Fields on Diffraction Peaks

Figure 2 shows the diffraction profile of a PZT-5H sample over a wide 2θ -range, indicating the pseudo-cubic peak locations. Figure 3 shows slow-scan diffraction profiles at pseudo-cubic (111), (200), and (220) regions in a depolarized sample at several applied electric field levels. It clearly shows that there exists a threshold electric field between $.33E_C$ to $.5E_C$ for all peaks. Below the threshold field, the diffraction profiles do not change. Experimental results show that the peaks at other pseudo-cubic regions behave in a similar way.

Figure 4 shows the change of the pseudo-cubic (200) peak in a polarized sample, where a positive electric field is along the poling direction. Unlike the case of a depolarized sample, there is no clear threshold electric field for peak profile change. Under a positive electric field, the change of diffraction profile is very small and gradual. Under a negative electric field, the peak profile changes slowly at low fields and profoundly when $|E| > 0.5E_C$. These observations are consistent with the value ($.5E_C$) observed by Wang et al., in which they applied an electric field perpendicular to the

poling direction and measured strains in both the poling direction and that normal to the poling direction²².

The fact that there exists a threshold value of electric field indicates that the residual stresses in PZT-5H play an important role in non-180° domain switching and phase change. In depolarized samples, residual stresses are relatively uniformly distributed throughout the material. Therefore, the threshold energy for domain switching and phase change in different grains is similar. Once such threshold energy level is reached upon an applied electric field, non-180° domain switching and phase transition occur. In a polarized sample, however, residual stress level differs profoundly from grain to grain and so is the threshold energy. Therefore, non-180° domain switching and phase transition in different grains/domains may be induced at different applied electric field levels, resulting in a continuous change in nonlinear piezoelectric constants^{15,16}.

Figure 5 shows pseudo-cubic (111) and (220) peaks in polarized samples. Under positive field, the magnitudes of the change are very small. However, the changes under negative electric fields are rather large. The nonlinear behavior of piezoelectric effects is found to depend on the direction of the applied electric field¹⁸. The strong direction-dependent peak profile changes shown in Figs. 4 and 5 are responsible for this nonlinear behavior. Moreover, it is interesting to find that around negative coercive field ($-0.8E_C$), a large profile change is induced by the electric field. The change corresponds to a large piezoelectric contraction and can explain the deep minima found in the strain-electric field hysteresis loop^{16,28}. It is commonly believed that a negative electric field induces 180° domain switching. However, our results in Fig.5 showed that, with magnitude below the coercive field, a negative electric field induces a large amount of non-180° domain

switching. This effect is likely due to the residual stresses generated during the poling process.

3.2 Fitting of Peaks

Because of the co-existence of morphotropic phases, each of the above pseudo-cubic diffraction peaks is composed of multiple peaks corresponding to different phases. Table 1 lists all the possible peaks at pseudo-cubic (111), (200), and (220) regions for tetragonal, rhombohedral and monoclinic phases in PZT-5H. In principle, all these phases, therefore the corresponding peaks, may be present in the material and thus within a particular pseudo-cubic peak. To study possible domain switching and phase transition, we conducted peak fitting to determine the individual peaks for different phases. We focused on the pseudo-cubic (111), (200), and (220) regions since other peaks would either contain too many individual peaks for different phases or have too low a 2θ angle to be very accurate.

We consider a mixture of two phases, either a mixture of tetragonal and rhombohedral phases or that of tetragonal and monoclinic phases. Practically, the number of individual peaks would be too large if we tried to fit the peaks to a mixture of three phases. Two methods are used in the fitting: one is to fit the individual peaks of the two phases to each of the three experimentally measured pseudo-cubic peaks; the other is to fit the individual peaks of the two phases to pseudo-cubic (220) peak to determine the lattice parameters of the two phases, and then use the lattice parameters to calculate the 2θ values of other peaks in the two phase mixture at pseudo-cubic (111) and (200) regions.

As seen in Table 1, for the pseudo-cubic (111), (200), and (220) peaks, we need to fit 3, 3, and 4 individual peaks for a mixture of tetragonal and rhombohedral phases; or 4, 4, and 6 peaks for a mixture of tetragonal and monoclinic phases, respectively. The fitted 2θ values of individual peaks are listed in the third column in Table 2, where T, R, and M stand for tetragonal, rhombohedral, and monoclinic phases.

With the second method mentioned above, by using the pseudo-cubic (220) peak, we minimized the low angle distortion effect. Moreover, there are enough peaks to determine all lattice parameters. The lattice parameters for a mixture of tetragonal and rhombohedral phases are determined as, tetragonal: $a = 4.0596\text{\AA}$, $c = 4.1158\text{\AA}$, Rhombohedral: $a = 4.0857\text{\AA}$, $\alpha = 89.668^\circ$; and those for a mixture of tetragonal and monoclinic phases, tetragonal: $a = 4.0595\text{\AA}$, $c = 4.1140\text{\AA}$, Monoclinic: $a_m = 5.7920\text{\AA}$, $b_m = 5.7541\text{\AA}$, $c_m = 4.0989\text{\AA}$, $\beta = 90.443^\circ$. The calculated peak positions at pseudo-cubic (111) and (200) directions using these lattice parameters are given in the second column in Table 2. It is clearly seen in Table 2 that the peaks positions obtained by these two methods agree with each other extremely well, rendering confidence in the current peak fitting methods and in the accuracy of the determined lattice parameters.

The results in Table 2 seem to suggest that both morphotropic phase compositions, i.e., mixture of tetragonal and rhombohedral phases or mixture of tetragonal and monoclinic phases, are possible compositions at room temperature. The current method is not able to determine which of these is the more likely microstructure of PZT-5H.

3.3 Effects of Electric Fields on Domain Switching and Phase Change

With the information on individual peak positions and intensities of different phases, we are now able to study the domain switching and phase change induced by the applied electric field. Figure 6 illustrates the fitted peaks at pseudo-cubic (200) region in a depolarized sample at $E = 0$ and $E = E_C$. Figure 6(a) shows the fitted peaks for a mixture of tetragonal and rhombohedral phases. It clearly shows that, as an electric field of E_C is applied, the intensity of T(002) increases while that of T(200) decreases, indicating 90° domain switching of tetragonal phase from the (200) to the (002) orientation. Moreover, the intensity of R(200) is decreased upon applied electric field, indicating a phase transition from rhombohedral to tetragonal, R(200) to T(002). Similar phenomenon is observed in Fig. 6(b) for a mixture of tetragonal and monoclinic phases. Upon applied electric field of E_C , there is a clear indication of 90° domain switching of the tetragonal phase from (200) to (002) orientation, and a phase change from M(220) to T(002). However, the intensity of the peak M(002) remains nearly the same upon applied electric field, indicating that this orientation is still the preferred one for the monoclinic phase upon applied electric field.

Results for the pseudo-cubic (200) peak of a polarized sample are given in Fig. 7. Figure 7(a) shows fitted peaks for a mixture of tetragonal and rhombohedral phases at 0, E_C , and $-0.8E_C$. The changes of the peak intensities indicate that, upon an applied electric field of E_C , 90° domain switching from T(200) to T(002) and phase transition from R(200) to T(002) are induced, but only in a very small amount. On the other hand, upon an electric field of $-0.8E_C$, 90° domain switching from T(002) to T(200) and phase transition from T(002) to R(200) are clearly induced in a large amount. Figure 7(b) shows

fitted peaks for a mixture of tetragonal and monoclinic phases at 0, E_C , and $-0.8E_C$. Upon an electric field of E_C , similar domain switching and phase transition behaviors as those observed in Fig. 6(b) are also induced in a polarized sample, but in a very small amount. Whereas upon an electric field of $-0.8E_C$, domain switching and phase transition in the opposite direction to those in Fig. 6(b) are induced in a large amount.

IV. CONCLUSIONS

Electric field induced domain switching and phase transition were studied using *in-situ* x-ray diffraction. Through the changes of x-ray diffraction profiles of pseudo-cubic peaks upon applied electric field, we identified when the switching and transition occur. Our results indicate that, for a depolarized PZT-5H sample, there exists a threshold field level below which little non-180° domain switching or phase transition occurs. This threshold value is significantly lower than the material's coercive field. In a polarized sample, on the other hand, no obvious threshold exists. When the applied electric field is in the same direction as the poling direction, the non-180° domain switching and phase change occur from a low electric field, although the switching and transition happen rather slowly as the applied electric field level increases. When the applied electric field is in the opposite direction from the poling direction, however, the changes are much more profound. These observations indicate that residual stresses in the material play an important role in inducing domain switching and phase change. The dependence of the non-180° domain switching and phase transition on the applied electric field in polarized materials is believed to be responsible for the electric field direction-dependent nonlinear piezoelectric behavior of PZT-5H.

Furthermore, by fitting the individual peaks of tetragonal, rhombohedral, and/or monoclinic phases to the measured pseudo-cubic (111), (200), and (220) peaks, we established that the material may be composed of a mixture of tetragonal and rhombohedral phases or a mixture of tetragonal and monoclinic phases. The peak fitting method also allows us to identify the electric field induced 90° domain switching in the tetragonal phase as well as the phase transitions between the tetragonal and rhombohedral phases or between the tetragonal and monoclinic phases.

ACKNOWLEDGEMENTS

This work has been supported by National Science Foundation Grant No: CMS 98-72306. The x-ray measurements were conducted at Frederick Seitz Materials Research Laboratory supported by DOE Grant DEFG02-91-ER45439.

REFERENCES

- ¹ B. Jaffe, W.R. Cook and H. Jaffe, *Piezoelectric Ceramics*, Academic Press, London, 1971.
- ² B. Noheda, D.E. Cox, G. Shirane, J.A. Gonzalo, L.E. Cross and S-E. Park, “A Monoclinic Ferroelectric Phase in the $\text{Pb}(\text{Zr}_{1-x}\text{Ti}_x)\text{O}_3$ Solid Solution”, *Appl. Phys. Lett.* **74**[14], 2059-61 (1999).
- ³ B. Noheda, J.A. Gonzalo, L.E. Cross, R. Guo, S-E. Park, D.E. Cox and G. Shirane, “Tetragonal-to-monoclinic Phase Transition in a Ferroelectric Perovskite: The Structure of $\text{PbZr}_{0.52}\text{Ti}_{0.48}\text{O}_3$,” *Phys. Rev. B* **61**[13], 8687-95 (2000).
- ⁴ B. Noheda, D.E. Cox, G. Shirane, R. Guo, B. Jones and L.E. Cross, “Stability of the Monoclinic Phase in the Ferroelectric Perovskite $\text{PbZr}_{1-x}\text{Ti}_x\text{O}_3$,” *Phys. Rev. B* **63**, 014103 (2000).
- ⁵ A.G. Souza Filho, K.C.V. Lima, A.P. Ayala, I. Guedes, P.T.C. Freire, J. Mendes Filho, E.B. Araújo and J.A. Eiras, “Monoclinic Phase of $\text{PbZr}_{0.52}\text{Ti}_{0.48}\text{O}_3$ Ceramics: Raman and Phenomenological Thermodynamic Studies,” *Phys. Rev. B* **61**[21], 14 283-86 (2000).
- ⁶ K.H. Yoon and H.R. Lee, “Electric-field-induced Strain and Piezoelectric Properties Near the Morphotropic Phase Boundary of $\text{Pb}(\text{Mg}_{1/3}\text{Nb}_{2/3})\text{O}_3$ - PbZrO_3 - PbTiO_3 Ceramics,” *J. Appl. Phys.* **89**[7], 3915-19 (2001).
- ⁷ H.D. Chen, K.R. Udayakumar, C.J. Gaskey, and L.E. Cross, “Electrical-Properties Maxima in Thin-Films of the Lead Zirconate Lead Titanate Solid-Solution System,” *Appl. Phys. Lett.* **67**[23], 3411-13 (1995).

- ⁸ H.Q. Fan and H-E. Kim, "Perovskite Stabilization and Electromechanical Properties of Polycrystalline Lead Zinc Niobate-Lead Zirconate Titanate," *J. Appl. Phys.* **91**[1], 317-21 (2001).
- ⁹ T.Y. Koo and S-W. Cheong, "Dielectric and Piezoelectric Enhancement Due to 90° Domain Rotation in the Tetragonal Phase of $\text{Pb}(\text{Mg}_{1/3}\text{Nb}_{2/3})\text{O}_3\text{-PbTiO}_3$," *Appl. Phys. Lett.* **80**[22], 4205-07 (2002).
- ¹⁰ S.K. Mishra, D. Pandey and A.P. Singh, "Effect of Phase Coexistence at Morphotropic Phase Boundary on the Properties of $\text{Pb}(\text{Zr}_{1-x}\text{Ti}_x)\text{O}_3$ Ceramics," *Appl. Phys. Lett.* **69**[12], 1707-09 (1996).
- ¹¹ R. Guo, L.E. Cross, S-E. Park, B. Noheda, D.E. Cox and G. Shirane, "Origin of the High Piezoelectric Response in $\text{PbZr}_{1-x}\text{Ti}_x\text{O}_3$," *Phys. Rev. Lett.* **84**[23], 5423-26 (2000).
- ¹² X.P. Li, W.Y. Shih, J.S. Vartuli and D.L. Milius, "Effect of a Transverse Tensile Stress on the Electric-field-induced Domain Reorientation in Soft PZT: In Situ XRD Study," *J. Am. Ceram. Soc.* **85**[4], 844-50 (2002).
- ¹³ S-F. Liu, S-E. Park, T.R. ShROUT and L.E. Cross, "Electric Field Dependence of Piezoelectric Properties for Rhombohedral $0.955\text{Pb}(\text{Zn}_{1/3}\text{Nb}_{2/3})\text{O}_3\text{-}0.045\text{PbTiO}_3$ Single Crystals," *J. Appl. Phys.* **85**[5], 2810-14 (1999).
- ¹⁴ D.A. Hall, "Review Nonlinearity in Piezoelectric Ceramics," *J. Mater. Res.* **36**, 4575-601 (2001).
- ¹⁵ Q.M. Zhang, W.Y. Pan, S.J. Jang, and L.E. Cross, "Domain Wall Excitations and their Contributions to the Weak-signal Response of Doped Lead Zirconate Titanate Ceramics," *J. Appl. Phys.*, **64**[11], 6445-51 (1988).

- ¹⁶ V.D. Kugel and L.E. Cross, "Behavior of Soft Piezoelectric Ceramics under High Sinusoidal Electric Fields," *J. Appl. Phys.* **84**[5], 2815-30 (1998).
- ¹⁷ V. Mueller and Q.M. Zhang, "Nonlinearity and Scaling Behavior in Donor-Doped Lead Zirconate Titanate," *Appl. Phys Lett.* **72**[21], 2692-94 (1998).
- ¹⁸ V. Perrin, M. Troccaz and P. Gonnard, "Nonlinear Behavior of the Permittivity and of the Piezoelectric Strain Constant Under High Electric Field Drive," *J. Electroceramics* **4**[1], 189-94 (2000).
- ¹⁹ M.K. Durbin, E.W. Jacobs, J.C. Hicks and S-E. Park, "In-situ X-ray Diffraction Study of an Electric Field Induced Phase Transition in the Single Crystal Relaxor Ferroelectric, 92%Pb(Zn_{1/3}Nb_{2/3})O₃-8%PbTiO₃," *Appl. Phys. Lett.* **74**[19], 2848-50 (1999).
- ²⁰ D-S. Paik, S-E. Park, S. Wada, S-F. Liu and T.R. Shrout, "E-field Induced Phase Transition in <001>-oriented Rhombohedral 0.92Pb(Zn_{1/3}Nb_{2/3})O₃-0.08PbTiO₃ Crystals," *J. Appl. Phys.* **85**[2], 1080-83 (1999).
- ²¹ H.X. Fu and R.E. Cohen, "Polarization Rotation Mechanism for Ultrahigh Electromechanical Response in Single-crystal Piezoelectrics," *Nature* **403**, 281-83 (2000).
- ²² D. Wang, Y. Fotinich and G.P. Carman, "Influence of Temperature on the Electromechanical and Fatigue Behavior of Piezoelectric Ceramics," *J. Appl. Phys.* **83**[10], 5342-50 (1998).
- ²³ S.M. Gupta and D. Viehland, "Tetragonal to Rhombohedral Transformation in the Lead Zirconium Titanate Lead Magnesium Niobate Lead Titanate Crystalline Solution," *J. Appl. Phys.* **83**[1], 407-14 (1998)

- ²⁴ W.W. Cao and L.E. Cross, "Theoretical Model for the Morphotropic Phase Boundary in Lead Zirconate-lead Titanate Solid Solution," *Phys. Rev. B* **47**[9], 4825-30 (1993).
- ²⁵ L. Bellaiche, A. Garcia and D. Vanderbilt, "Finite-temperature Properties of $\text{Pb}(\text{Zr}_{1-x}\text{Ti}_x)\text{O}_3$ Alloys from First Principles," *Phys. Rev. Lett.* **84**[23], 5427-30 (2000).
- ²⁶ L. Bellaiche, A. Garcia and D. Vanderbilt, "Electric-field Induced Polarization Paths in $\text{Pb}(\text{Zr}_{1-x}\text{Ti}_x)\text{O}_3$ Alloys," *Phys. Rev. B* **64**, 060103 (2001).
- ²⁷ R. W. Cheary and A. A. Coelho, *Programs XFIT and FOURYA, deposited in CCP14 Powder Diffraction Library*, Engineering and Physical Sciences Research Council, Daresbury Laboratory, Warrington, England (1996).
- ²⁸ D. Viehland, J. Powers, L. Ewart, and J.F. Li, "Ferroelastic Switching and Elastic Nonlinearity in $\langle 001 \rangle$ -Oriented $\text{Pb}(\text{Mg}_{1/3}\text{Nb}_{2/3})\text{O}_3$ - PbTiO_3 and $\text{Pb}(\text{Zn}_{1/3}\text{Nb}_{2/3})\text{O}_3$ - PbTiO_3 Crystals," *J. Appl. Phys.* **88**[8], 4907-09 (2001).

Table 1. Peaks at pseudo-cubic (111), (200), and (220) regions

Pseudo-cubic	(111)	(200)	(220)
Tetragonal	(111)	(002), (200)	(202), (220)
Rhombohedral	(111), ($\bar{1}\bar{1}1$)	(200)	(220), ($\bar{2}\bar{2}0$)
Monoclinic	($\bar{2}01$), (021), (201)	(002), (220)	($\bar{2}22$), (222), (400), (040)

Table 2. Fitted and computed peaks at pseudo-cubic (111), (200), and (220) regions

(Wavelength $K\alpha_1$: 1.5406 Å)

Tetragonal and Rhombohedral			Tetragonal and Monoclinic		
Peak	Computed $2\theta(^{\circ})$	Fitted $2\theta(^{\circ})$	Peak	Computed $2\theta(^{\circ})$	Fitted $2\theta(^{\circ})$
R(111)	37.892	37.936	M($\bar{2}01$)	37.871	37.936
T(111)	38.194	38.114	M(201)	38.158	38.114
R($1\bar{1}1$)	38.197	38.114	M(021)	38.187	38.114
T(002)	43.964	43.967	T(111)	38.200	38.114
R(020)	44.306	44.271	T(002)	43.984	43.920
T(200)	44.605	44.516	M(002)	44.156	44.129
R(220)*	64.246	64.246	M(220)	44.347	44.362
T(202)*	64.422	64.422	T(200)	44.606	44.539
R($\bar{2}20$)*	64.662	64.662	M($\bar{2}22$)*	64.172	64.172
T(220)*	64.917	64.917	M(400)*	64.280	64.280
			T(202)*	64.438	64.438
			M(222)*	64.565	64.565
			M(040)*	64.753	64.753
			T(220)*	64.919	64.919
Lattice Parameters: Tetragonal: $a = 4.0596\text{Å}$, $c = 4.1158\text{Å}$; Rhombohedral: $a = 4.0857\text{Å}$, $\alpha = 89.668^{\circ}$			Lattice Parameters: Tetragonal: $a = 4.0595\text{Å}$, $c = 4.1140\text{Å}$; Monoclinic: $a_m = 5.7920\text{Å}$, $b_m = 5.7541\text{Å}$, $c_m = 4.0989\text{Å}$, $\beta = 90.443^{\circ}$		

* Peaks used to calculated lattice parameters

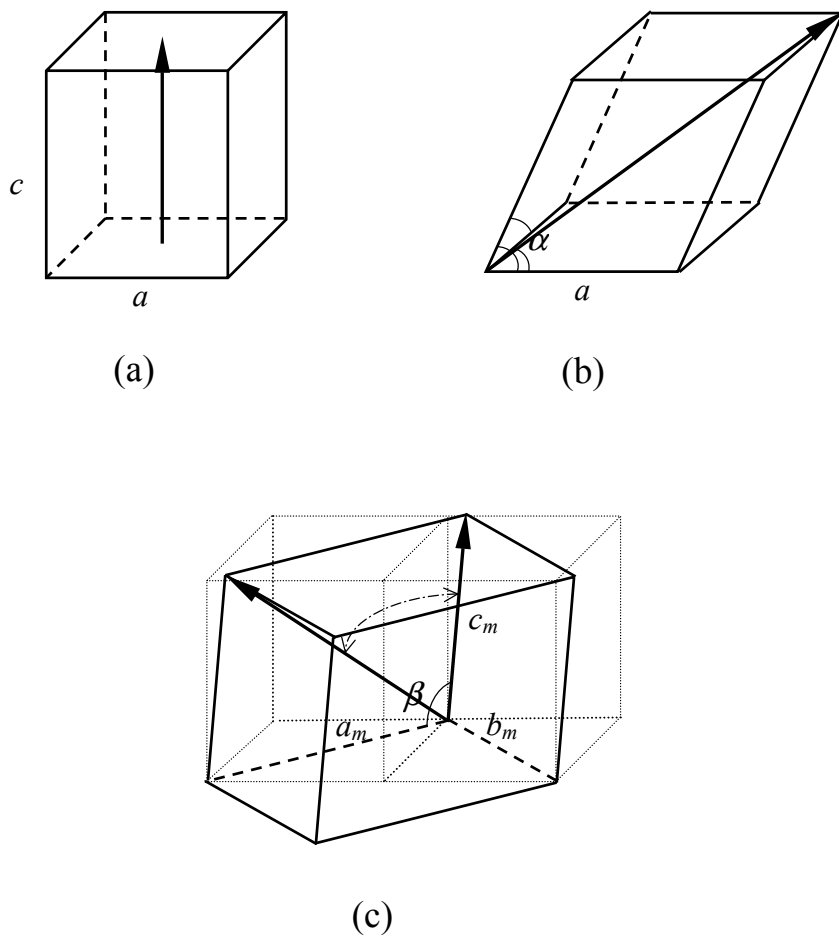


Fig. 1 Unit cells of individual phases in PZT: (a) tetragonal, (b) rhombohedral, (c) monoclinic.

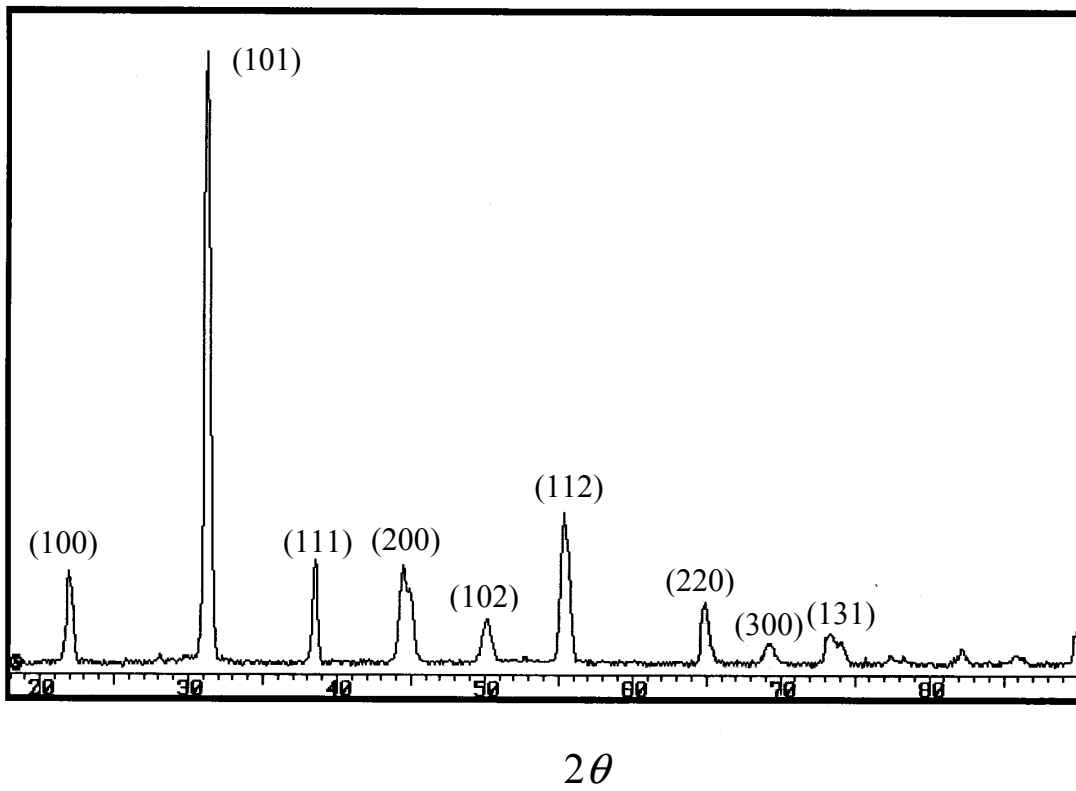


Fig. 2 Diffraction profile of a polarized sample.

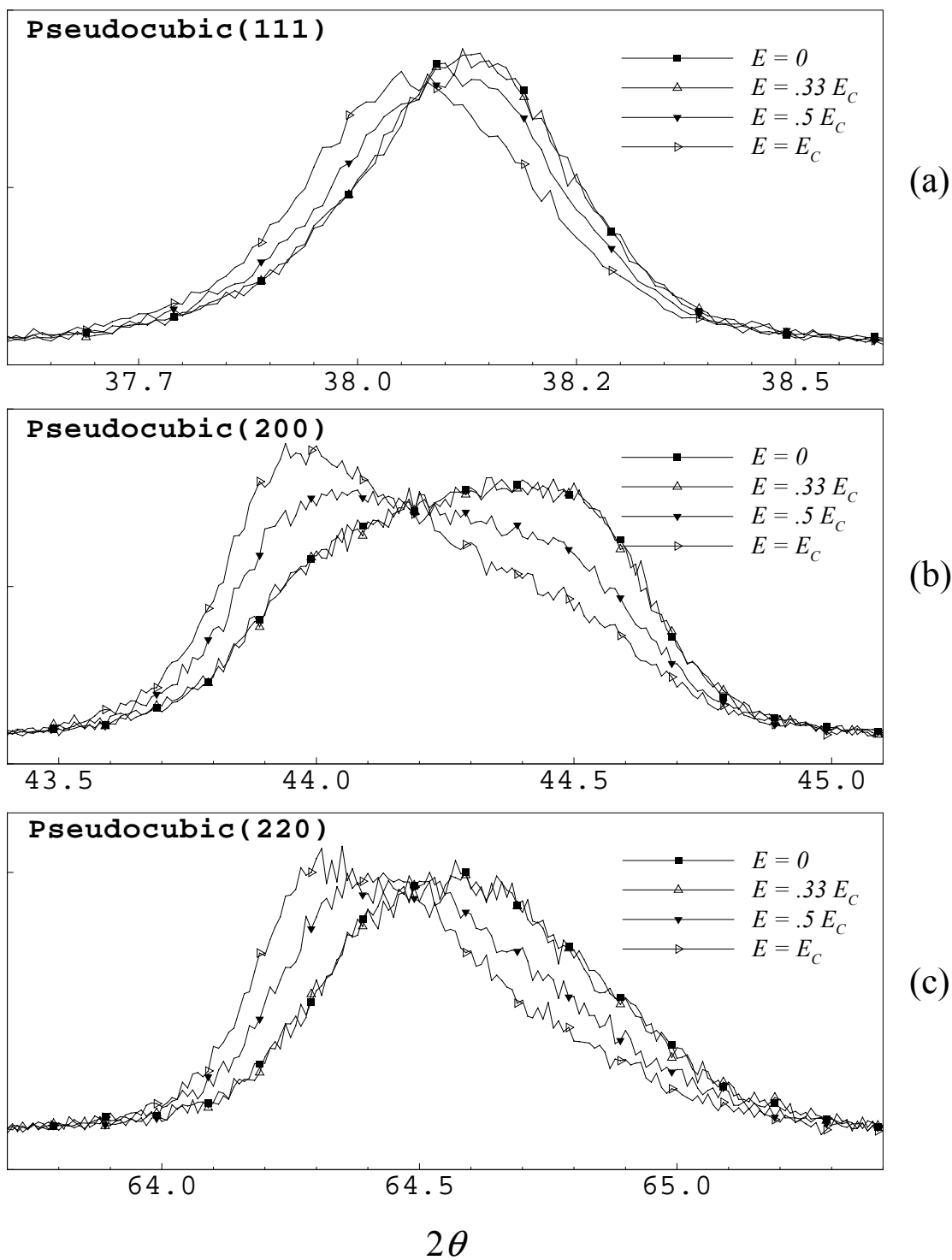


Fig. 3 Pseudo-cubic peaks of a depolarized sample under several positive electric field

levels: (a) (111) peak, (b) (200) peak, (c) (220) peak.

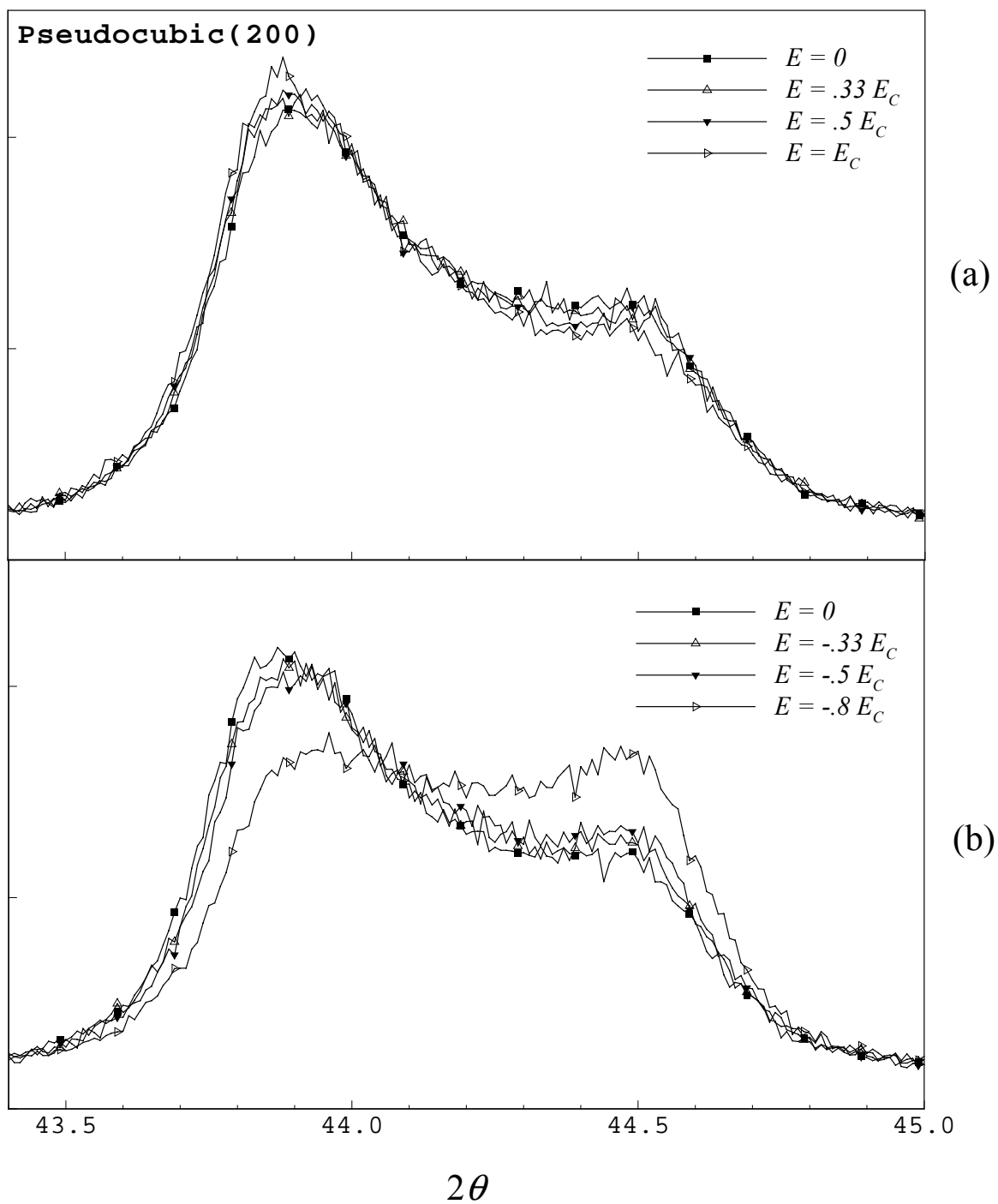


Fig. 4 Pseudo-cubic (200) peak of a polarized sample: (a) under different positive electric field levels, (b) under different negative electric field levels.

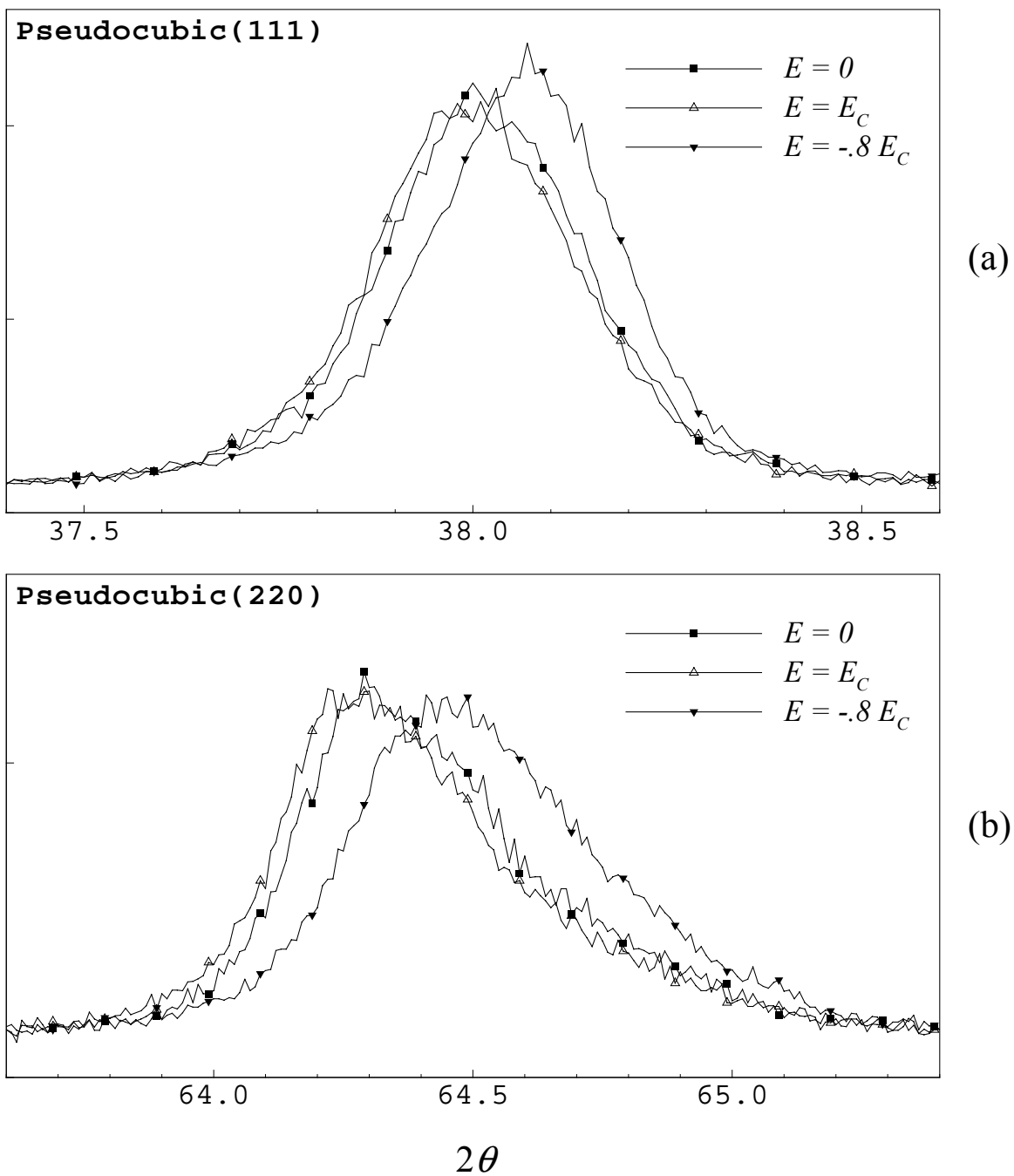


Fig. 5 Pseudo-cubic (111) and (220) peaks of a polarized sample under zero, a positive, and a negative electric fields: (a) (111) peak, (b) (220) peak.

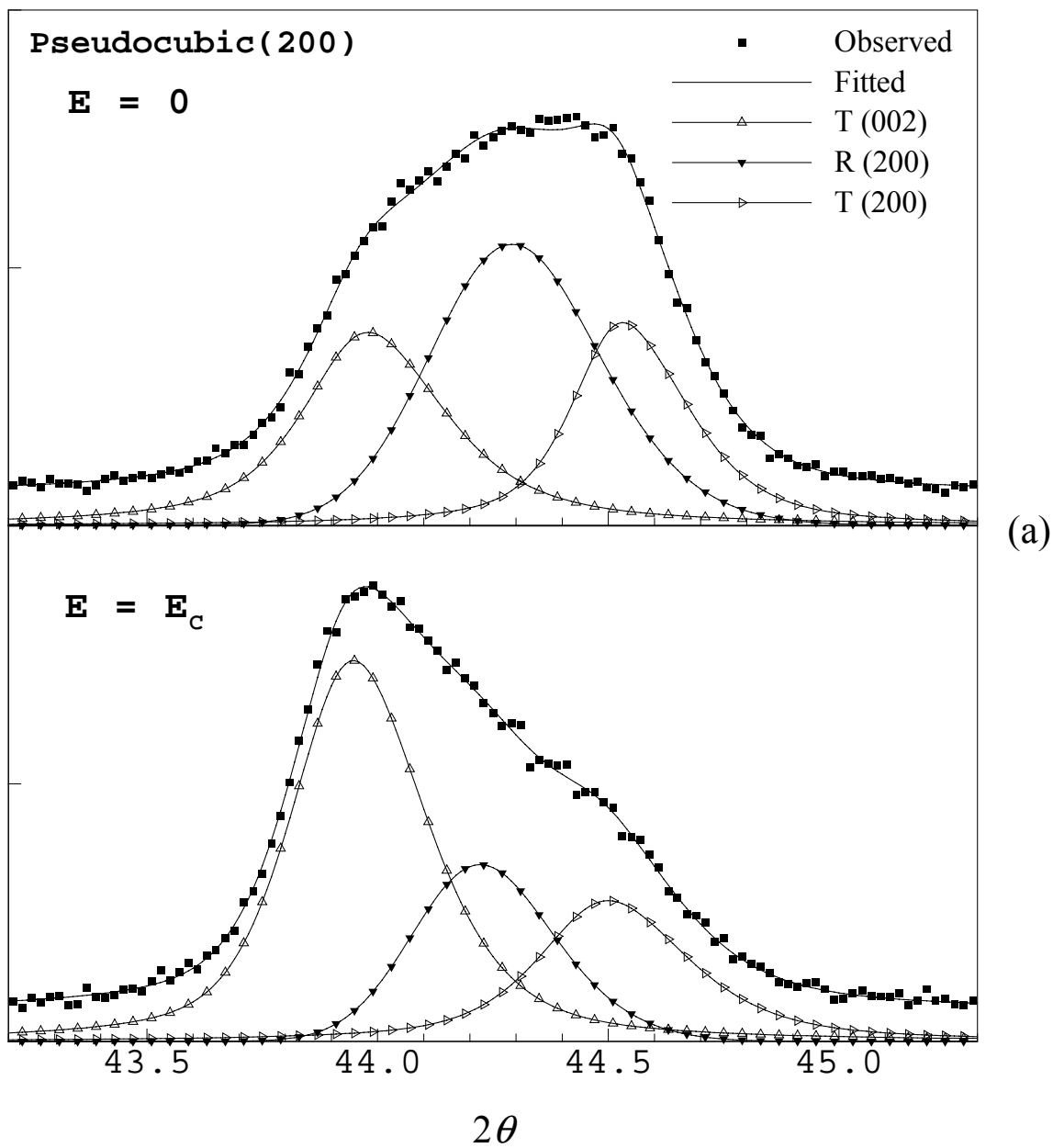


Fig. 6 Fitted peaks at pseudo-cubic (200) region of a depolarized sample: (a) mixture of tetragonal and rhombohedral phases

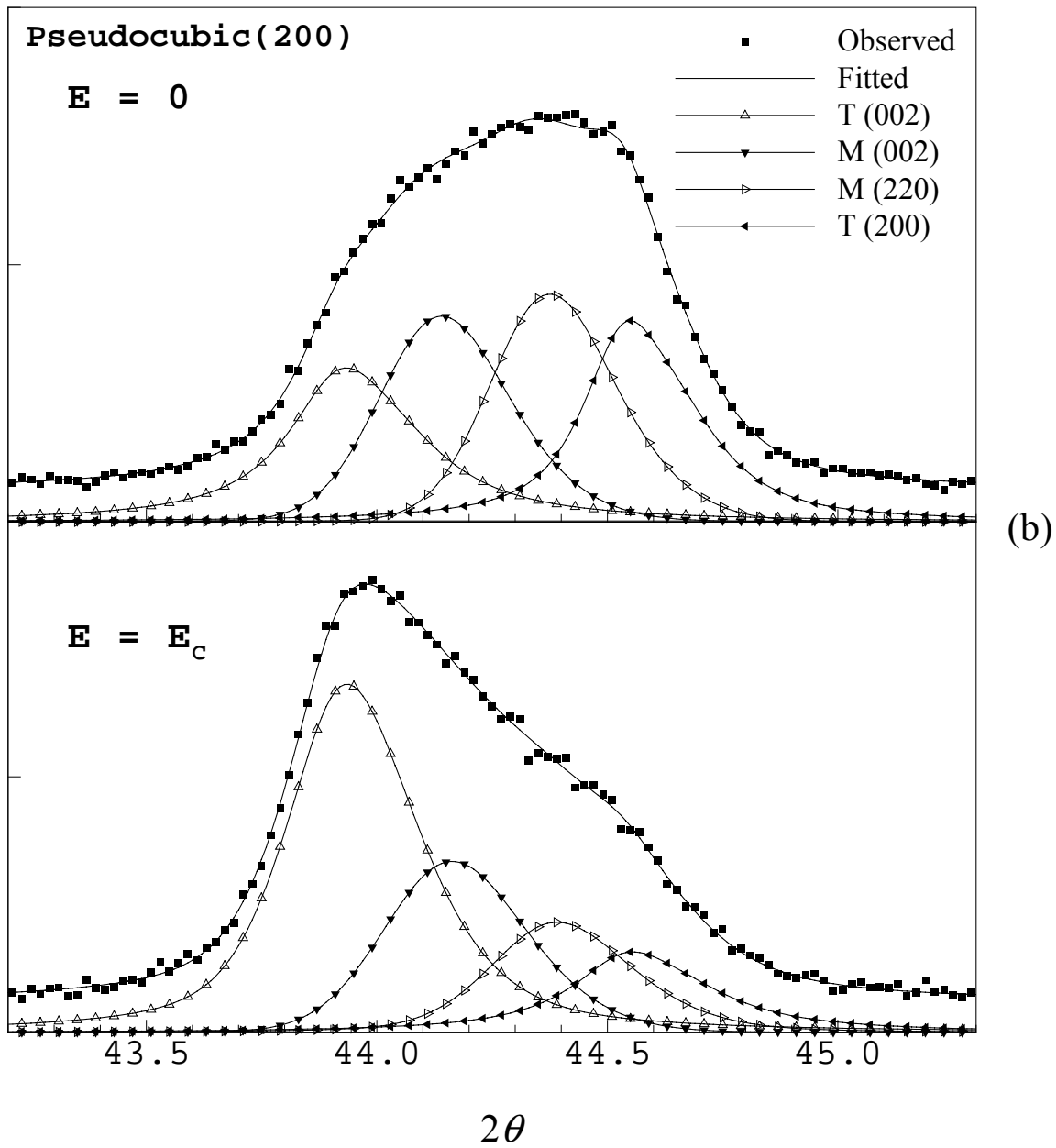


Fig. 6 (Cont'd) Fitted peaks at pseudo-cubic (200) region of a depolarized sample: (b) mixture of tetragonal and monoclinic phases.

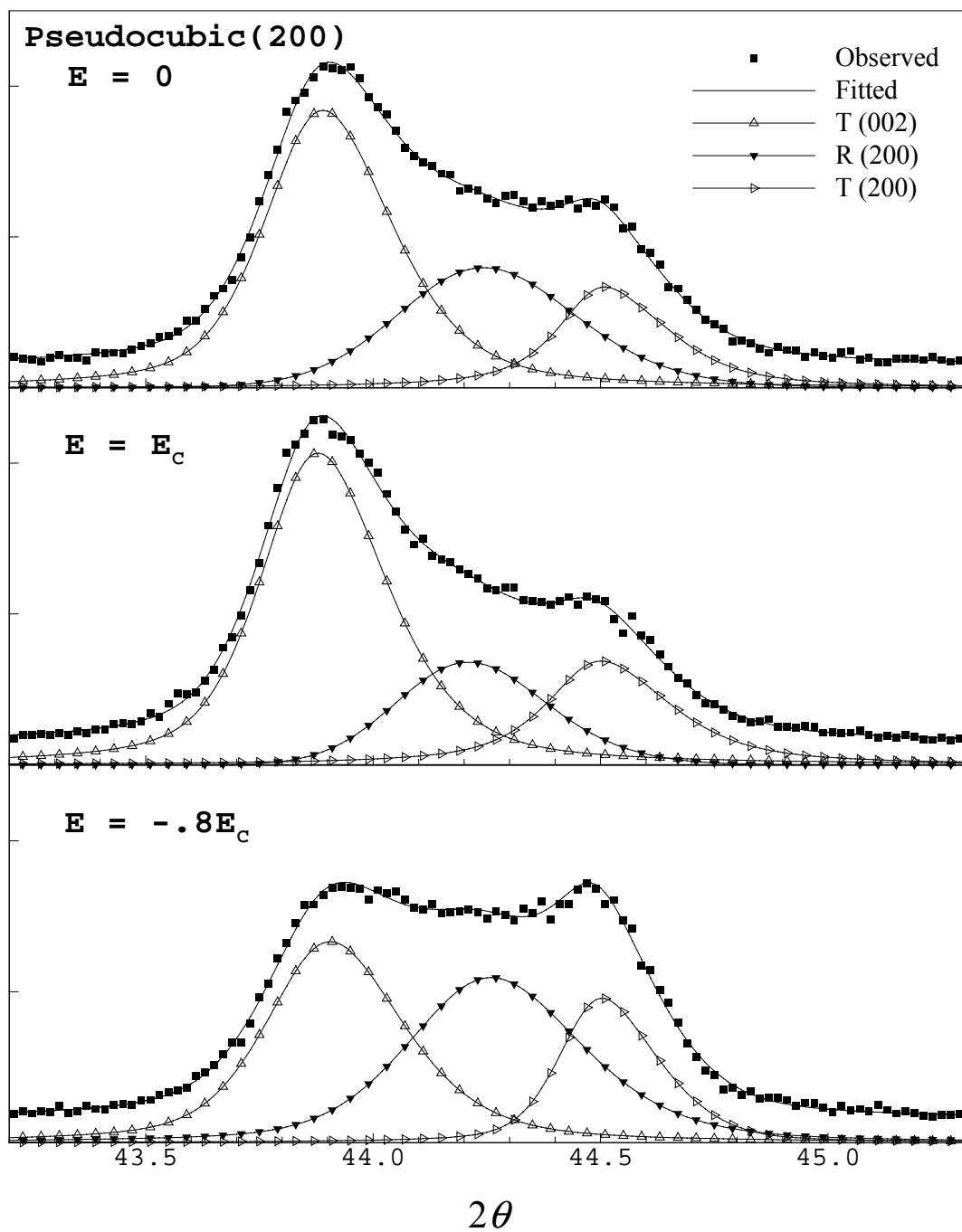
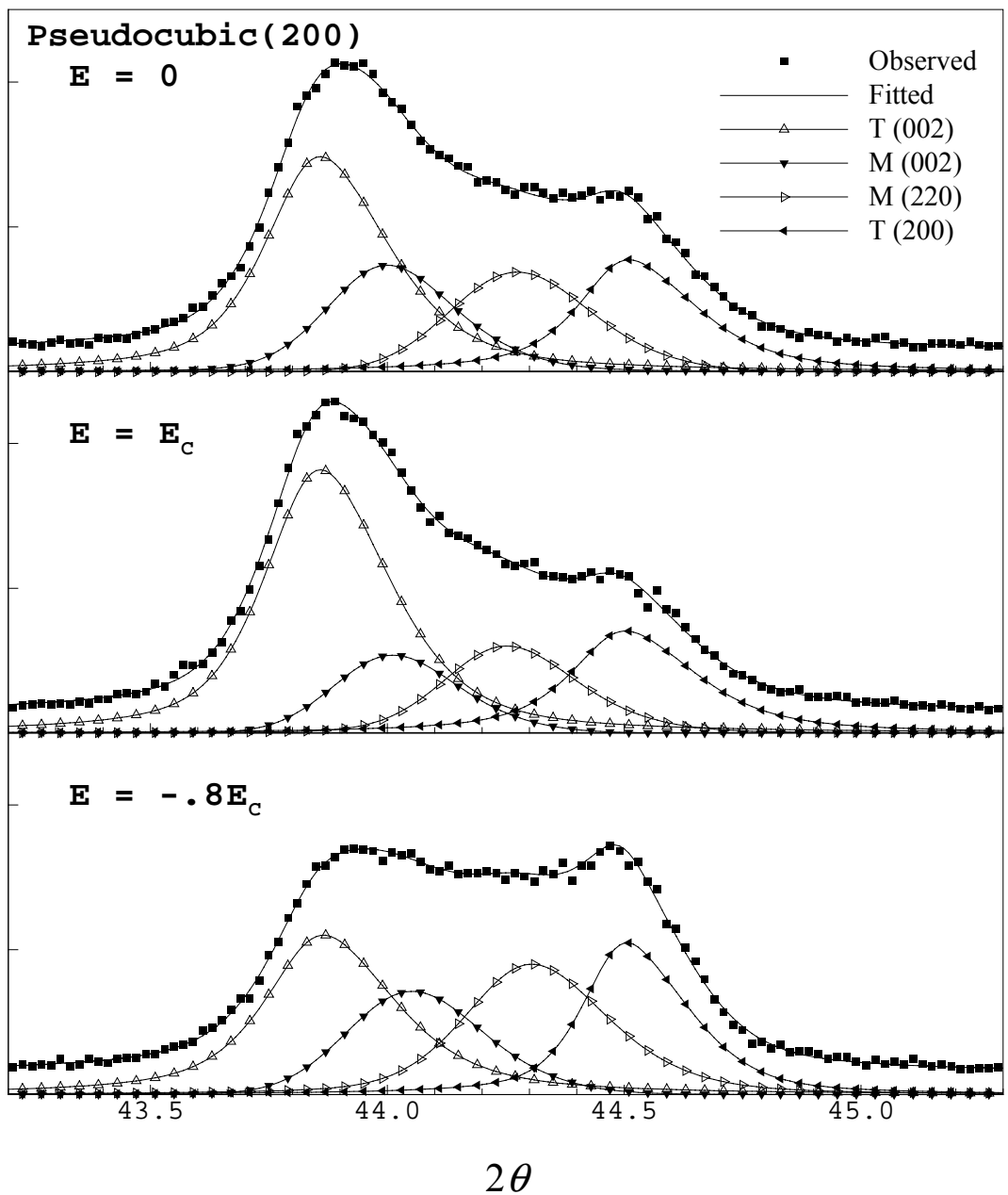


Fig. 7 Fitted peaks at pseudo-cubic (200) region of a polarized Sample: (a) mixture of tetragonal and rhombohedral phases



(b)

Fig. 7 (Cont'd) Fitted peaks at pseudo-cubic (200) region of a polarized Sample: (b) mixture of tetragonal and monoclinic phases.

List of Recent TAM Reports

No.	Authors	Title	Date
942	Riahi, D. N.	Non-axisymmetric chimney convection in a mushy layer under a high-gravity environment – In <i>Centrifugal Materials Processing</i> (L. L. Regel and W. R. Wilcox, eds.), 295–302 (2001)	May 2000
943	Christensen, K. T., S. M. Soloff, and R. J. Adrian	PIV Sleuth: Integrated particle image velocimetry interrogation/validation software	May 2000
944	Wang, J., N. R. Sottos, and R. L. Weaver	Laser induced thin film spallation – <i>Experimental Mechanics</i> (submitted)	May 2000
945	Riahi, D. N.	Magneto-hydrodynamic effects in high gravity convection during alloy solidification – In <i>Centrifugal Materials Processing</i> (L. L. Regel and W. R. Wilcox, eds.), 317–324 (2001)	June 2000
946	Gioia, G., Y. Wang, and A. M. Cuitiño	The energetics of heterogeneous deformation in open-cell solid foams – <i>Proceedings of the Royal Society of London A</i> 457 , 1079–1096 (2001)	June 2000
947	Kessler, M. R., and S. R. White	Self-activated healing of delamination damage in woven composites – <i>Composites A: Applied Science and Manufacturing</i> 32 , 683–699 (2001)	June 2000
948	Phillips, W. R. C.	On the pseudomomentum and generalized Stokes drift in a spectrum of rotational waves – <i>Journal of Fluid Mechanics</i> 430 , 209–229 (2001)	July 2000
949	Hsui, A. T., and D. N. Riahi	Does the Earth's nonuniform gravitational field affect its mantle convection? – <i>Physics of the Earth and Planetary Interiors</i> (submitted)	July 2000
950	Phillips, J. W.	Abstract Book, 20th International Congress of Theoretical and Applied Mechanics (27 August – 2 September, 2000, Chicago)	July 2000
951	Vainchtein, D. L., and H. Aref	Morphological transition in compressible foam – <i>Physics of Fluids</i> 13 , 2152–2160 (2001)	July 2000
952	Chaïeb, S., E. Sato- Matsuo, and T. Tanaka	Shrinking-induced instabilities in gels	July 2000
953	Riahi, D. N., and A. T. Hsui	A theoretical investigation of high Rayleigh number convection in a nonuniform gravitational field – <i>International Journal of Pure and Applied Mathematics</i> , in press (2003)	Aug. 2000
954	Riahi, D. N.	Effects of centrifugal and Coriolis forces on a hydromagnetic chimney convection in a mushy layer – <i>Journal of Crystal Growth</i> 226 , 393–405 (2001)	Aug. 2000
955	Fried, E.	An elementary molecular-statistical basis for the Mooney and Rivlin–Saunders theories of rubber-elasticity – <i>Journal of the Mechanics and Physics of Solids</i> 50 , 571–582 (2002)	Sept. 2000
956	Phillips, W. R. C.	On an instability to Langmuir circulations and the role of Prandtl and Richardson numbers – <i>Journal of Fluid Mechanics</i> 442 , 335–358 (2001)	Sept. 2000
957	Chaïeb, S., and J. Sutin	Growth of myelin figures made of water soluble surfactant – Proceedings of the 1st Annual International IEEE-EMBS Conference on Microtechnologies in Medicine and Biology (October 2000, Lyon, France), 345–348	Oct. 2000
958	Christensen, K. T., and R. J. Adrian	Statistical evidence of hairpin vortex packets in wall turbulence – <i>Journal of Fluid Mechanics</i> 431 , 433–443 (2001)	Oct. 2000
959	Kuznetsov, I. R., and D. S. Stewart	Modeling the thermal expansion boundary layer during the combustion of energetic materials – <i>Combustion and Flame</i> , in press (2001)	Oct. 2000
960	Zhang, S., K. J. Hsia, and A. J. Pearlstein	Potential flow model of cavitation-induced interfacial fracture in a confined ductile layer – <i>Journal of the Mechanics and Physics of Solids</i> , 50 , 549–569 (2002)	Nov. 2000
961	Sharp, K. V., R. J. Adrian, J. G. Santiago, and J. I. Molho	Liquid flows in microchannels – Chapter 6 of <i>CRC Handbook of MEMS</i> (M. Gad-el-Hak, ed.) (2001)	Nov. 2000

List of Recent TAM Reports (cont'd)

No.	Authors	Title	Date
962	Harris, J. G.	Rayleigh wave propagation in curved waveguides – <i>Wave Motion</i> 36 , 425–441 (2002)	Jan. 2001
963	Dong, F., A. T. Hsui, and D. N. Riahi	A stability analysis and some numerical computations for thermal convection with a variable buoyancy factor – <i>Journal of Theoretical and Applied Mechanics</i> 2 , 19–46 (2002)	Jan. 2001
964	Phillips, W. R. C.	Langmuir circulations beneath growing or decaying surface waves – <i>Journal of Fluid Mechanics</i> (submitted)	Jan. 2001
965	Bdzil, J. B., D. S. Stewart, and T. L. Jackson	Program burn algorithms based on detonation shock dynamics – <i>Journal of Computational Physics</i> (submitted)	Jan. 2001
966	Bagchi, P., and S. Balachandar	Linearly varying ambient flow past a sphere at finite Reynolds number: Part 2 – Equation of motion – <i>Journal of Fluid Mechanics</i> (submitted)	Feb. 2001
967	Cermelli, P., and E. Fried	The evolution equation for a disclination in a nematic fluid – <i>Proceedings of the Royal Society A</i> 458 , 1–20 (2002)	Apr. 2001
968	Riahi, D. N.	Effects of rotation on convection in a porous layer during alloy solidification – Chapter 12 in <i>Transport Phenomena in Porous Media</i> (D. B. Ingham and I. Pop, eds.), 316–340 (2002)	Apr. 2001
969	Damljanovic, V., and R. L. Weaver	Elastic waves in cylindrical waveguides of arbitrary cross section – <i>Journal of Sound and Vibration</i> (submitted)	May 2001
970	Gioia, G., and A. M. Cuitiño	Two-phase densification of cohesive granular aggregates – <i>Physical Review Letters</i> 88 , 204302 (2002) (in extended form and with added co-authors S. Zheng and T. Uribe)	May 2001
971	Subramanian, S. J., and P. Sofronis	Calculation of a constitutive potential for isostatic powder compaction – <i>International Journal of Mechanical Sciences</i> (submitted)	June 2001
972	Sofronis, P., and I. M. Robertson	Atomistic scale experimental observations and micromechanical/continuum models for the effect of hydrogen on the mechanical behavior of metals – <i>Philosophical Magazine</i> (submitted)	June 2001
973	Pushkin, D. O., and H. Aref	Self-similarity theory of stationary coagulation – <i>Physics of Fluids</i> 14 , 694–703 (2002)	July 2001
974	Lian, L., and N. R. Sottos	Stress effects in ferroelectric thin films – <i>Journal of the Mechanics and Physics of Solids</i> (submitted)	Aug. 2001
975	Fried, E., and R. E. Todres	Prediction of disclinations in nematic elastomers – <i>Proceedings of the National Academy of Sciences</i> 98 , 14773–14777 (2001)	Aug. 2001
976	Fried, E., and V. A. Korchagin	Striping of nematic elastomers – <i>International Journal of Solids and Structures</i> 39 , 3451–3467 (2002)	Aug. 2001
977	Riahi, D. N.	On nonlinear convection in mushy layers: Part I. Oscillatory modes of convection – <i>Journal of Fluid Mechanics</i> 467 , 331–359 (2002)	Sept. 2001
978	Sofronis, P., I. M. Robertson, Y. Liang, D. F. Teter, and N. Aravas	Recent advances in the study of hydrogen embrittlement at the University of Illinois – Invited paper, Hydrogen–Corrosion Deformation Interactions (Sept. 16–21, 2001, Jackson Lake Lodge, Wyo.)	Sept. 2001
979	Fried, E., M. E. Gurtin, and K. Hutter	A void-based description of compaction and segregation in flowing granular materials – <i>Proceedings of the Royal Society of London A</i> (submitted)	Sept. 2001
980	Adrian, R. J., S. Balachandar, and Z.-C. Liu	Spanwise growth of vortex structure in wall turbulence – <i>Korean Society of Mechanical Engineers International Journal</i> 15 , 1741–1749 (2001)	Sept. 2001
981	Adrian, R. J.	Information and the study of turbulence and complex flow – <i>Japanese Society of Mechanical Engineers Journal B</i> , in press (2002)	Oct. 2001
982	Adrian, R. J., and Z.-C. Liu	Observation of vortex packets in direct numerical simulation of fully turbulent channel flow – <i>Journal of Visualization</i> , in press (2002)	Oct. 2001
983	Fried, E., and R. E. Todres	Disclinated states in nematic elastomers – <i>Journal of the Mechanics and Physics of Solids</i> 50 , 2691–2716 (2002)	Oct. 2001
984	Stewart, D. S.	Towards the miniaturization of explosive technology – Proceedings of the 23rd International Conference on Shock Waves (2001)	Oct. 2001

List of Recent TAM Reports (cont'd)

No.	Authors	Title	Date
985	Kasimov, A. R., and Stewart, D. S.	Spinning instability of gaseous detonations – <i>Journal of Fluid Mechanics</i> (submitted)	Oct. 2001
986	Brown, E. N., N. R. Sottos, and S. R. White	Fracture testing of a self-healing polymer composite – <i>Experimental Mechanics</i> (submitted)	Nov. 2001
987	Phillips, W. R. C.	Langmuir circulations – <i>Surface Waves</i> (J. C. R. Hunt and S. Sajjadi, eds.), in press (2002)	Nov. 2001
988	Gioia, G., and F. A. Bombardelli	Scaling and similarity in rough channel flows – <i>Physical Review Letters</i> 88 , 014501 (2002)	Nov. 2001
989	Riahi, D. N.	On stationary and oscillatory modes of flow instabilities in a rotating porous layer during alloy solidification – <i>Journal of Porous Media</i> , in press (2002)	Nov. 2001
990	Okhuysen, B. S., and D. N. Riahi	Effect of Coriolis force on instabilities of liquid and mushy regions during alloy solidification – <i>Physics of Fluids</i> (submitted)	Dec. 2001
991	Christensen, K. T., and R. J. Adrian	Measurement of instantaneous Eulerian acceleration fields by particle-image accelerometry: Method and accuracy – <i>Experimental Fluids</i> (submitted)	Dec. 2001
992	Liu, M., and K. J. Hsia	Interfacial cracks between piezoelectric and elastic materials under in-plane electric loading – <i>Journal of the Mechanics and Physics of Solids</i> 51 , 921–944 (2003)	Dec. 2001
993	Panat, R. P., S. Zhang, and K. J. Hsia	Bond coat surface rumpling in thermal barrier coatings – <i>Acta Materialia</i> 51 , 239–249 (2003)	Jan. 2002
994	Aref, H.	A transformation of the point vortex equations – <i>Physics of Fluids</i> 14 , 2395–2401 (2002)	Jan. 2002
995	Saif, M. T. A, S. Zhang, A. Haque, and K. J. Hsia	Effect of native Al ₂ O ₃ on the elastic response of nanoscale aluminum films – <i>Acta Materialia</i> 50 , 2779–2786 (2002)	Jan. 2002
996	Fried, E., and M. E. Gurtin	A nonequilibrium theory of epitaxial growth that accounts for surface stress and surface diffusion – <i>Journal of the Mechanics and Physics of Solids</i> , in press (2002)	Jan. 2002
997	Aref, H.	The development of chaotic advection – <i>Physics of Fluids</i> 14 , 1315–1325 (2002); see also <i>Virtual Journal of Nanoscale Science and Technology</i> , 11 March 2002	Jan. 2002
998	Christensen, K. T., and R. J. Adrian	The velocity and acceleration signatures of small-scale vortices in turbulent channel flow – <i>Journal of Turbulence</i> , in press (2002)	Jan. 2002
999	Riahi, D. N.	Flow instabilities in a horizontal dendrite layer rotating about an inclined axis – <i>Proceedings of the Royal Society of London A</i> , in press (2003)	Feb. 2002
1000	Kessler, M. R., and S. R. White	Cure kinetics of ring-opening metathesis polymerization of dicyclopentadiene – <i>Journal of Polymer Science A</i> 40 , 2373–2383 (2002)	Feb. 2002
1001	Dolbow, J. E., E. Fried, and A. Q. Shen	Point defects in nematic gels: The case for hedgehogs – <i>Proceedings of the National Academy of Sciences</i> (submitted)	Feb. 2002
1002	Riahi, D. N.	Nonlinear steady convection in rotating mushy layers – <i>Journal of Fluid Mechanics</i> , in press (2003)	Mar. 2002
1003	Carlson, D. E., E. Fried, and S. Sellers	The totality of soft-states in a neo-classical nematic elastomer – <i>Proceedings of the Royal Society A</i> (submitted)	Mar. 2002
1004	Fried, E., and R. E. Todres	Normal-stress differences and the detection of disclinations in nematic elastomers – <i>Journal of Polymer Science B: Polymer Physics</i> 40 , 2098–2106 (2002)	June 2002
1005	Fried, E., and B. C. Roy	Gravity-induced segregation of cohesionless granular mixtures – <i>Lecture Notes in Mechanics</i> , in press (2002)	July 2002
1006	Tomkins, C. D., and R. J. Adrian	Spanwise structure and scale growth in turbulent boundary layers – <i>Journal of Fluid Mechanics</i> (submitted)	Aug. 2002

List of Recent TAM Reports (cont'd)

No.	Authors	Title	Date
1007	Riahi, D. N.	On nonlinear convection in mushy layers: Part 2. Mixed oscillatory and stationary modes of convection— <i>Journal of Fluid Mechanics</i> (submitted)	Sept. 2002
1008	Aref, H., P. K. Newton, M. A. Stremmer, T. Tokieda, and D. L. Vainchtein	Vortex crystals— <i>Advances in Applied Mathematics</i> 39 , in press (2002)	Oct. 2002
1009	Bagchi, P., and S. Balachandar	Effect of turbulence on the drag and lift of a particle— <i>Physics of Fluids</i> (submitted)	Oct. 2002
1010	Zhang, S., R. Panat, and K. J. Hsia	Influence of surface morphology on the adhesive strength of aluminum/epoxy interfaces— <i>Journal of Adhesion Science and Technology</i> (submitted)	Oct. 2002
1011	Carlson, D. E., E. Fried, and D. A. Tortorelli	On internal constraints in continuum mechanics— <i>Journal of Elasticity</i> (submitted)	Oct. 2002
1012	Boyland, P. L., M. A. Stremmer, and H. Aref	Topological fluid mechanics of point vortex motions— <i>Physica D</i> 175 , 69-95 (2002)	Oct. 2002
1013	Bhattacharjee, P., and D. N. Riahi	Computational studies of the effect of rotation on convection during protein crystallization— <i>Journal of Crystal Growth</i> (submitted)	Feb. 2003
1014	Brown, E. N., M. R. Kessler, N. R. Sottos, and S. R. White	<i>In situ</i> poly(urea-formaldehyde) microencapsulation of dicyclopentadiene— <i>Journal of Microencapsulation</i> (submitted)	Feb. 2003
1015	Brown, E. N., S. R. White, and N. R. Sottos	Microcapsule induced toughening in a self-healing polymer composite— <i>Journal of Materials Science</i> (submitted)	Feb. 2003
1016	Kuznetsov, I. R., and D. S. Stewart	Burning rate of energetic materials with thermal expansion— <i>Combustion and Flame</i> (submitted)	Mar. 2003
1017	Dolbow, J., E. Fried, and H. Ji	Chemically induced swelling of hydrogels— <i>Journal of the Mechanics and Physics of Solids</i> (submitted)	Mar. 2003
1018	Costello, G. A.	Mechanics of wire rope—Mordica Lecture, Interwire 2003, Wire Association International, Atlanta, Georgia, May 12, 2003	Mar. 2003
1019	Wang, J., N. R. Sottos, and R. L. Weaver	Thin film adhesion measurement by laser induced stress waves— <i>Journal of the Mechanics and Physics of Solids</i> (submitted)	Apr. 2003
1020	Bhattacharjee, P., and D. N. Riahi	Effect of rotation on surface tension driven flow during protein crystallization— <i>Microgravity Science and Technology</i> (submitted)	Apr. 2003
1021	Fried, E.	The configurational and standard force balances are not always statements of a single law— <i>Proceedings of the Royal Society</i> (submitted)	Apr. 2003
1022	Panat, R. P., and K. J. Hsia	Experimental investigation of the bond coat rumpling instability under isothermal and cyclic thermal histories in thermal barrier systems— <i>Proceedings of the Royal Society of London A</i> (submitted)	May 2003
1023	Fried, E., and M. E. Gurtin	A unified treatment of evolving interfaces accounting for small deformations and atomic transport: grain-boundaries, phase transitions, epitaxy— <i>Advances in Applied Mechanics</i> (submitted)	May 2003
1024	Dong, F., D. N. Riahi, and A. T. Hsui	On similarity waves in compacting media— <i>Advances in Mathematics Research</i> (submitted)	May 2003
1025	Liu, M., and K. J. Hsia	Locking of electric field induced non-180° domain switching and phase transition in ferroelectric materials upon cyclic electric fatigue— <i>Applied Physics Letters</i> (submitted)	May 2003
1026	Liu, M., K. J. Hsia, and M. Sardela Jr.	<i>In situ</i> X-ray diffraction study of electric field induced domain switching and phase transition in PZT-5H— <i>Journal of the American Ceramics Society</i> (submitted)	May 2003